https://doi.org/10.3311/PPch.37050

Periodica Polytechnica Chemical Engineering, 68(3), pp. 437–445, 2024

Experimental Investigation and Specific Heat Capacity Prediction of Graphene Nanoplatelet-Infused SAE10W Oil Using Artificial Neural Networks

Sekar Manikandan[1*], Adhinarayanapuram Jayaram Devanathan Nanthakumar[1]

[1] Department of Automobile Engineering, College of Engineering and Technology, SRM Institute of Science and Technology, Kattankulathur Campus, 603203 Chengalpattu, Tamilnadu, India
[*] Corresponding author, e-mail: manimech14625@gmail.com

Received: 04 April 2024, Accepted: 17 June 2024, Published online: 02 August 2024

Abstract

This research aims to develop an artificial neural network (ANN) model to predict the specific heat capacity (SHC) of graphene/SAE10W oil nanofluid. An experimental investigation of the SHC of graphene nanoplatelets infused in SAE10W oil was carried out using a thermal constant analyzer. In experimental testing the volume percentage and fluid temperature range vary from 0.05 to 0.15 and 293 K to 353 K, respectively. The experimental data shows the graphene/SAE10W oil nanofluid exhibited a reduction in SHC relative to the base fluid. The ANN model was developed using experimental data to predict the specific heat capacity of graphene/SAE10W oil nanofluid. During ANN model training, the correlation coefficient and mean square error of 0.999 and 6.592×10^{-6} were achieved, respectively. Compared to experimental values, the ANN model predicts SHC with a 0.45 error percentage. Additionally, a mathematical model has been developed to predict the SHC of graphene/SAE10W oil nanofluids using curve fitting. The data obtained from the developed mathematical model showed excellent correlation with all experimental values, with an error percentage of ±0.42. Hence, it is concluded that both models provide an optimal approach for estimating their SHC.

Keywords

graphene nanoplatelets, nanofluids, specific heat capacity, artificial neural network, correlation

1 Introduction

In many industrial sectors, energy transportation for cooling and heating persists as a challenge. Traditional fluids are commonly used by these industries to facilitate energy transfer within thermal systems. The inefficiency of heat transfer in traditional fluids like water, ethylene glycol (EG), and mineral oils is often due to their lower thermal conductivity [1–3]. Therefore, enhancing traditional fluids' heat transfer capability is highly desirable. In recent years, nanotechnology progress has resulted in the advent of nanofluids (NFs), a new type of heat transfer fluid. These NFs are solid-liquid blends consisting of solid nanoparticles smaller than 100 nm and a conventional fluid. Nanoparticles can be made from a variety of materials, including metals, metal oxides, non-metallic substances, and carbon nanotubes [4]. The potential for NFs to improve heat transfer and energy efficiency in a wide range of applications is immense [5, 6].

The applications of NFs to thermal systems have garnered considerable attention from researchers, particularly due to their crucial role in energy conversion. There are many applications for NFs in thermal systems, including solar collectors [7], microelectronics [8], aerospace [9], automotive [10], and heat exchangers [11], among others [12, 13]. Several properties of NFs are particularly relevant to various applications, including density, viscosity, thermal conductivity, specific heat capacity (SHC), and diffusivity. These properties determine the flow characteristics and heat transfer capabilities of NFs. Since then, researchers have extensively investigated the thermophysical properties of NFs.

Azharuddin et al. [14] investigated the thermophysical properties of hybrid NFs composed of $AgNO_3$-graphene and water at concentrations (Φ) between 0.01 and 0.03 v/v%. They found that adding 0.01%, 0.02%, and 0.03% hybrid NFs to base fluids raised the thermal conductivity by 8.21%, 15.37%, and 23.59% at 348 K, respectively, compared to base fluids. Conversely, SHC decreased by 0.011%, 0.027%, and 0.042% for Φ of 0.01 v/v%, 0.02 v/v%, and 0.03 v/v% at 348 K, respectively. Rubaiee et al. [15] found that incorporating graphene oxide nanoparticles with EG

Cite this article as: Manikandan, S., Nanthakumar, A. J. D. "Experimental Investigation and Specific Heat Capacity Prediction of Graphene Nanoplatelet-Infused SAE10W Oil Using Artificial Neural Networks", Periodica Polytechnica Chemical Engineering, 68(3), pp. 437–445, 2024.
https://doi.org/10.3311/PPch.37050

and water mixture nanofluid significantly increased their thermal conductivity by 9.5% at 313 K.

The properties of NFs, such as thermal conductivity and viscosity, have received the most attention, while density and SHC have received considerably less attention. Thermal diffusivity and conductivity can also be calculated using SHC to determine an NFs heat storage capacity. The SHC of NFs has been investigated in several experimental studies [16–18]. Although experimental measurements are a reliable method for measuring the SHC of NFs, the process of synthesizing and characterizing them can be costly and technically difficult. The use of models and simulation studies can help in addressing these challenges. In previous studies, theoretical models have not been able to accurately predict the SHC of NFs. As a result, a more precise estimate of SHC requires an alternative approach. In this regard, machine learning (ML) techniques, such as artificial neural networks (ANN), have been used to investigate the thermophysical properties of various NFs. For instance, Zhang et al. [19] investigated and developed a Gaussian process regression model (GPR) to predict the SHC of NFs. The model utilized a dataset comprising CuO and Al_2O_3 nanoparticles, along with water and EG as base liquids. They observed that the developed model exhibited a high correlation coefficient of 99.99% and demonstrated high prediction accuracy.

Mukesh Kumar et al. [20] created a GPR model to predict the thermal conductivity and dynamic viscosity ratios of NFs made of Al_2O_3 and water. The model showed that the thermal conductivity ratio and the dynamic viscosity ratio were very close to the experimental data, with root mean square error (RMSE) values of 0.000126 and 0.000045, respectively. Kamsuwan et al. [21] analyzed three major types of water-based nanoparticles, including Al_2O_3, CuO, and TiO_2, using an ANN model. They found that the predictions of the NF properties using the ANN model matched reality better than other numerical methods. There was only a 4.1% maximum error in the predicted results. Wang et al. [22] developed the ANN model to predict the thermal conductivity of NFs containing EG and various nanoparticles. The model showed a high correlation between the predicted results and experimental data, with 99.74% of the data within 5% of their respective deviations. Similarly, Shaopeng Tian et al. [23] investigated and created an ANN model to predict the thermal conductivity of a graphene oxide-Al_2O_3/water-EG hybrid nanofluid. They discovered that the ANN model has an average mean square error (MSE) of 1.67×10^{-6} and a correlation coefficient of 0.999. Sharma et al. [24] utilized ML algorithms to analyze the thermal conductivity of Titania water NFs. The findings revealed that gradient boosting emerged as the most effective algorithm for thermal conductivity predictions, achieving test and train accuracy of 99%. Ibrahim et al. [25] developed an ANN and RSM model to figure out how well SiO_2-EG and SiO_2-glycerol NFs conduct heat. Both methods were able to accurately predict the thermal conductivity ratio, and a cubic function with an R^2 value of 0.9977 and 0.9994, respectively, was suggested for both NFs. Similarly, Tawfeeq Abdullah Alkanhal [26] examined the thermal conductivity of reduced graphene oxide solids dispersed in water. The study revealed that the highest enhancement in thermal conductivity (31.19%) was observed at a concentration of 5 m/m% at 323 K. By curve-fitting the 3D output, a novel correlation was developed, predicting nanofluid thermal conductivity with a minimum deviation of 1.25%. Additionally, an artificial neural network was trained, achieving an R^2 value of 0.99. Olumegbon et al. [27] created a machine learning model that could predict the viscosity of carbon nanomaterials in diesel oil. The model was able to achieve a 99.98% correlation coefficient and a 99.99% RMSE for both the training and testing data sets. Meijuan et al. [28] developed the ANN model to estimate the thermophysical properties of magnetic NFs with an average deviation of 5% based on experimental data. However, only a few studies have used ANN to predict the SHC of NFs.

Similarly, the novelty of the work is the incorporation of graphene nanoplatelets into SAE10W oil for enhancing automotive shock absorber performance. In addition, the utilization of ANN for predicting the SHC of graphene/SAE10W oil NFs adds an innovative approach for the integration of advanced computational techniques in material science. We developed an ANN and mathematical models to estimate the SHC of these NFs. The effectiveness of ANN and mathematical models in predicting the SHC of graphene/SAE10W oil NFs was evaluated by comparing experimental data with predictions obtained from the developed models.

2 Materials and methods

2.1 Experimental data collection

In this study, graphene nanoplatelets (thickness 4 nm, length 2 μm, purity ≥ 99.0%, surface area of 700 m^2/g, density at 293 K is 2100 kg/m^3) procured from Cheap Tubes Inc., (USA) were utilized in the preparation of the NFs, with automotive shock absorber oil (Make: India Yamaha Motor PVT. Ltd, grade: SAE10W) selected as the base fluid. The density of SAE10W oil, determined at 293 K, is 875.5 kg/m^3 using a pycnometer in accordance with ASTM D1298. Fig. 1 shows a high-resolution scanning electron microscopic image (HRSEM, ThermoScientific Apreo S) used for characterizing

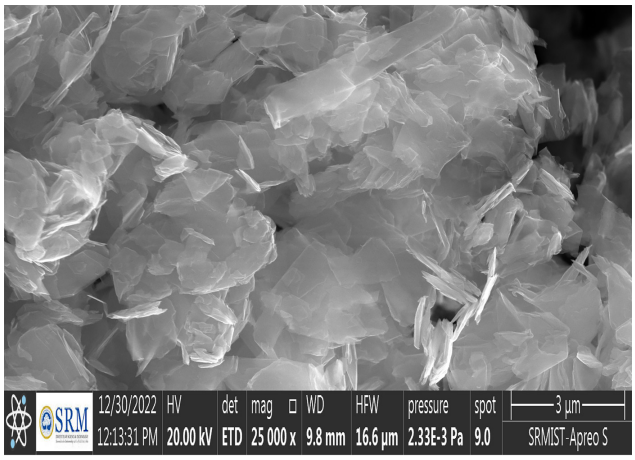

Fig. 1 HRSEM micrograph of graphene nanoplatelets

the morphological properties of graphene nanoplatelets. These images reveal that the graphene nanoplatelets are thin sheets with wrinkled surfaces. Furthermore, a two-step procedure [21] were used to prepare NFs with a uniform distribution of nanoparticles, which ensures that the nanoparticles are evenly distributed throughout the base fluid.

The thermal constants analyzer from Hot Disk Instrument (Model: TPS2500S) was used to measure the SHC of the graphene/SAE10W oil NFs. In this experiment, graphene nanoplatelet was influenced by Φ variation and the fluid temperature (T) ranged from 293 K to 353 K. The mass of graphene nanoplatelets was calculated using Eq. (1).

$$m_{\text{graphene}} = \left[\frac{\Phi}{100-\Phi}\right]\left[\frac{\rho_{\text{graphene}}}{\rho_{SAE10\,\text{Woil}}}\right] m_{SAE10\,\text{Woil}} \quad (1)$$

In this equation ρ_{graphene} is the density of graphene nanoparticles (kg/m^3), $\rho_{\text{SAE10Woil}}$ represents the density of the oil in (kg/m^3), m_{graphene} represents the mass of the graphene nanoparticles in g, while $m_{\text{SAE10Woil}}$ indicates the mass of the oil in g.

2.2 Development of ANN and mathematical models

ANNs are computational models that are constructed by replicating biologically inspired neural networks and their structures and functions. The nonlinear data pattern can be learned by ANNs by using a model network to provide better output. There are three layers in the ANN model, with different numbers of neurons in each layer. Its input neurons on the first layer transmit data to the hidden layer located on the second layer, and the output neurons on the third layer form the output layer. Neurons are interconnected across all layers via a mass coefficient. The schematic layout of ANN structure and applications of the NFs are shown in Fig. 2. The data processing process involves iterative refinement of successive outputs until the difference between them is minimized to improve data quality. The configuration information for the ANN structure is shown in Table 1.

For estimating the SHC of graphene/SAE10W oil NFs, a multi-layer perceptron (MLP)–ANN model was developed using NNTOOL in MATLAB software [29]. The Levenberg-Marquardt (Trainlm) backpropagation algorithm, considered as one of the best methods for training an ANN, was also utilized. For modeling the ANN, a single hidden layer feed-forward MLP method was selected. Tan-Sigmoid and purelin were selected as the active transfer functions for both the hidden and output layers. The ANN used 65 experimental data points, with T and Φ being inputs and SHC values being outputs. The model used three sets of data inputs categorized as training, validation and testing. Specifically, the training set comprised 45 (70%) of the 65 experimental SHC data points, while the validation and test sets included 10 (15%) of the 65 data points each. The most suitable

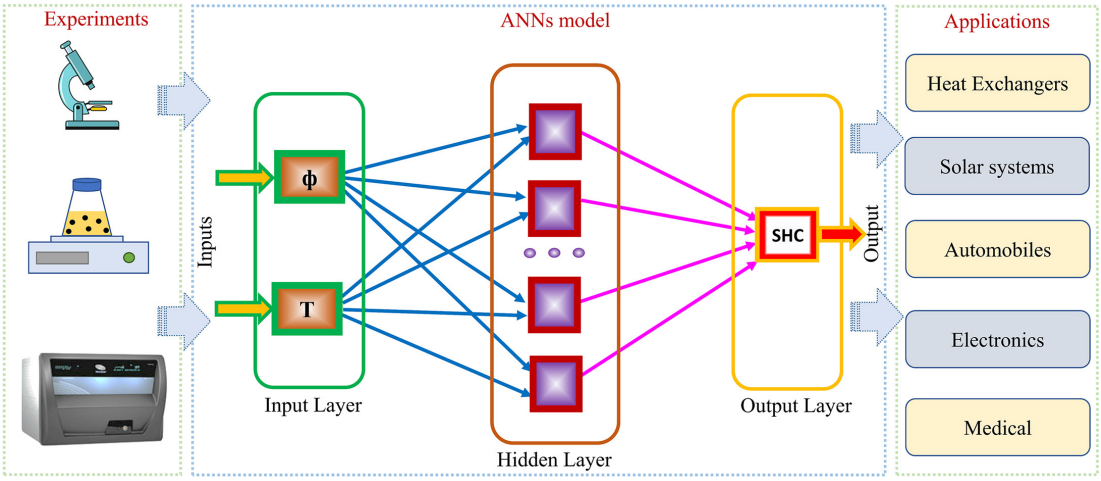

Fig. 2 ANN structure schematic layout for predicting SHC of NFs and NFs applications

Table 1 The ANN structure information

Network Parameters	Information
Neural network structure	Multi-layer perceptron
Type of network	Feed forward
Training approach	Back propagation
Error criteria	MSE & *R*
Best training method	Trainlm
Number of hidden layers	1
Hidden layer activation function	Tan-Sig
Output layer function	Purelin
Number of training data	45
Number of validation data	10
Number of test data	10

architecture and ANN design capable of predicting the results optimally were determined by varying the number of neurons in the hidden layer.

When simulations are performed with different quantities of neurons in the hidden layer, different outcomes may occur. Consequently, a simulation was conducted using various numbers of neurons to ascertain the optimal quantity, which was found to be 7. A comparison between the simulation iteration was made to determine the most suitable architecture. The flowchart for determining the optimal ANN model is illustrated in Fig. 3. To optimize the ANN, the MSE value in Eq. (2) and the *R* value in Eq. (3) were employed [30]. These criteria show that the constructed ANN model accurately estimates the SHC of the graphene/SAE10W oil NFs.

$$MSE = \frac{1}{N}\sum_{i=1}^{N}\left(C_{P_{\exp\,(i)}} - C_{P_{ANN\,(i)}}\right)^2 \tag{2}$$

$$R = \sqrt{1 - \frac{\sum_{i=1}^{N}\left(C_{P_{\exp\,(i)}} - C_{P_{ANN\,(i)}}\right)^2}{\sum_{i=1}^{N}\left(C_{P_{\exp\,(i)}}\right)^2}} \tag{3}$$

In the above equations, N denotes the total number of data points, and $C_{P(\exp)}$ represents the SHC value measured through experimentation. $C_{P(ANN)}$ represents the SHC value derived from the ANN model.

A mathematical model was built to estimate the SHC with the help of experimental data and curve fitting application of MATLAB software. This technique is considered to change the order of polynomial equations to form mathematical correlations that are dependent on the sum of squared errors (SSE) and R^2 values. The resulting mathematical model predicts the SHC of the graphene/SAE10W oil NFs based on Φ and *T*.

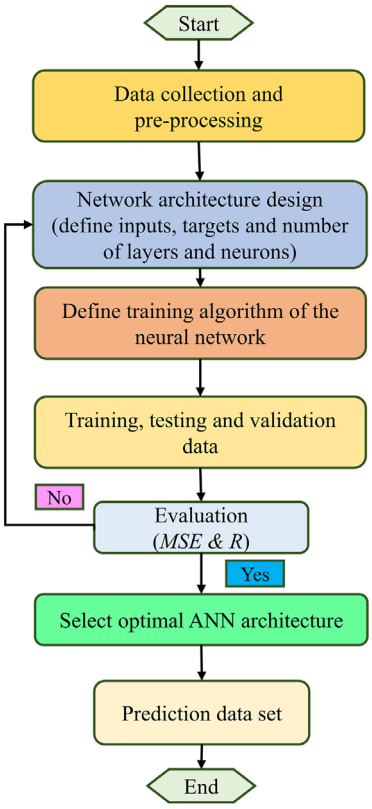

Fig. 3 Flowchart of the proposed algorithm for optimizing ANNs

3 Result and discussion

3.1 Experimental analysis of SHC of NFs

ANN models were built based on 65 data points from graphene/SAE10W oil NFs at five different Φ levels. The SHC values of the base fluid and graphene/SAE10W oil NFs are shown in Fig. 4.

The T range from 293 K to 353 K, and the Φ values are 0.050, 0.075, 0.100, 0.125, and 0.150 v/v%. As shown in the figure, the *x*-axis represents the Φ of graphene nanoplatelets, while the *y*-axis represents the SHC of fluids.

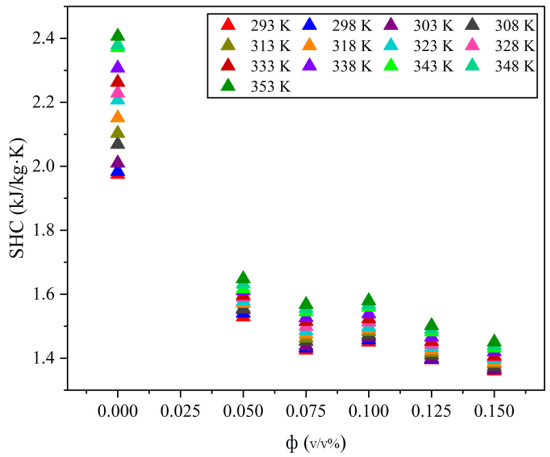

Fig. 4 SHC of graphene/SAE10W oil NFs

This figure indicates the SHC of the base fluid oil increases from 1.97 kJ/kg K to 2.41 kJ/kg K with an increase in *T*. However, when nanoparticles are added, the SHC of the base fluid gradually decreases. The minimum and maximum reductions in SHC of the graphene/SAE10W oil NFs relative to the base fluid are 19% at 293 K with a graphene Φ of 0.050 v/v% and 40% at 353 K with a graphene Φ of 0.150 v/v%, respectively. Typically, fluids exhibit higher SHC than metals. This is because metals have tightly packed atoms that can efficiently conduct heat from one atom to another atom [31, 32]. As a result, metals require significantly less energy per unit mass to heat than fluids. The transfer of heat through conduction, which is aided by convection, is primarily done by NFs when nanoparticle concentrations increases. As a result of this transition, the SHC of NFs decreases. Furthermore, a high volume per surface area could result in an increase or decrease in SHC [33].

3.2 ANN model performance analysis

In the training process of an ANN, the performance chart is a significant indicator, especially when predicting SHC, as depicted in Fig. 5. This graph illustrates the changes in MSE as training progresses. The horizontal axis represents the number of repetitions (epochs) in the training loop, while the vertical axis represents the MSE. In the early stages, MSE values are high, but they decrease after repeated training. In Fig. 5, the training curve continuously decreases and reaches its best validation point at epoch 52, with an MSE value of 6.592×10^{-6}.

The trainlm algorithm optimal ANN is identified by altering the number of neurons in the hidden layers during the process. The output functions are approximated by selecting the network with the least error. Another indicator of proper ANN training is the regression diagram and regression coefficient (*R*) between the actual ANN output data and the experimental data, respectively. In Fig. 6 the training, validation, testing, and overall segments of the ANN are presented. As shown in these figures, there is a close correlation between the experimental results and predictions. The results show the ANN was trained accurately and was able to predict nanofluid SHC. The *R* indicates the relationship between experimental and ANN prediction values. The *R* value of 1 signifies a close relationship between the experimental and prediction data, although zero suggests an accidental relationship. According to the findings, the *R* for all segments of the ANN are greater than 0.9996, indicating a strong correlation between the experimental and prediction data.

A histogram of ANN errors for an SHC parameter is depicted and presented in bar chart format as shown in Fig. 7. The figure indicates, the instances of errors across different error values. The *x*-axis shows the error values, while the frequency or number of errors related to each value is shown on the *y*-axis. A low error rate within the system is indicated by repeated occurrences of data errors near the zero-error line, which indicates well-trained problem data. Taller bar charts near the zero-error line, indicate a higher numerical density, which signifies the

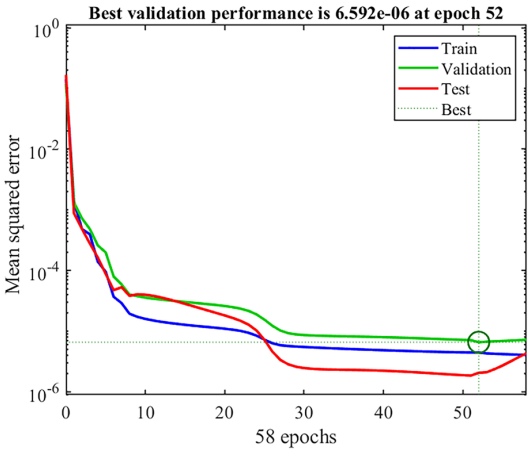

Fig. 5 Variations of epochs with MSE

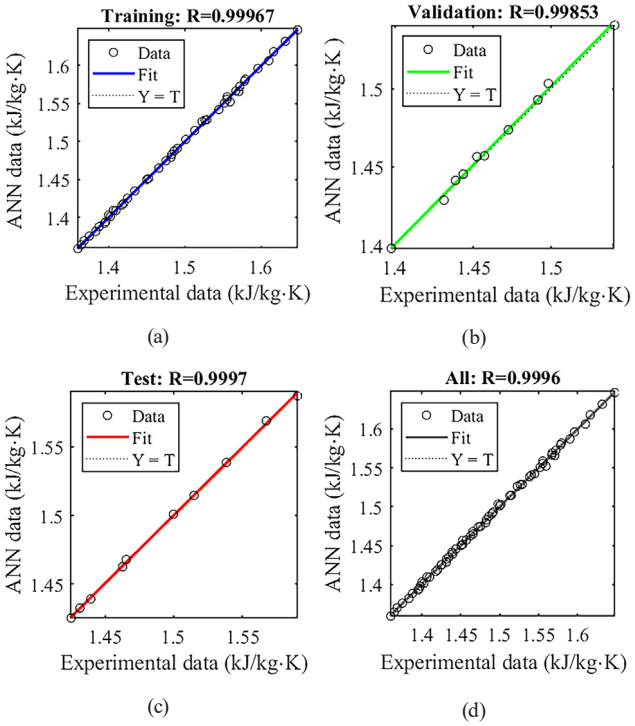

Fig. 6 Regression diagram for ANN prediction: a), training, b) validation, c) testing d) overall

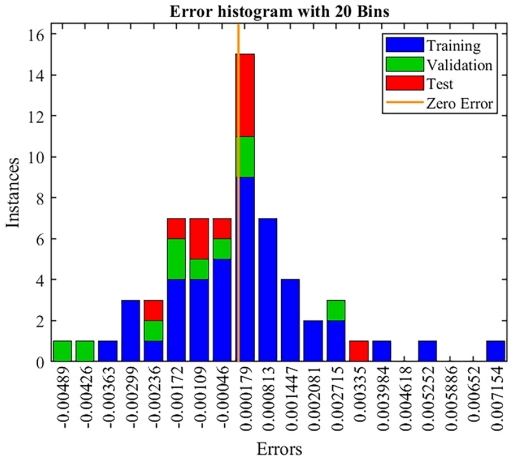

Fig. 7 ANN error histogram

selected method has effectively brought the output of predicted ANN values very close to the experimental values.

3.3 Mathematical model performance analysis

In Figs. 8 and 9, two-dimensional contour plots and three-dimensional surface plots illustrate every possible interaction parameter that can influence SHC, respectively. A mathematical model was used to determine the optimal performance of the graphene/SAE10W oil NFs.

In this approach, polynomials ranging from first to fourth order is employed to predict the output variable.

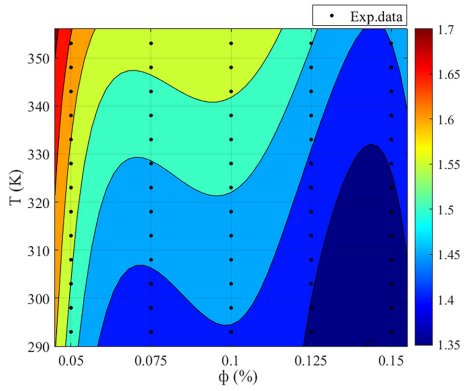

Fig. 8 Contour plots for SHC of NFs

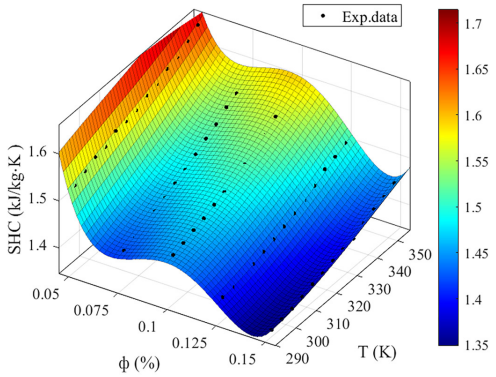

Fig. 9 Surface fit plots for SHC of NFs

These polynomials comprise a combination of linear equations and are expressed in Eq. (4) as follows:

$$\frac{(C_p)_{nf}}{(C_p)_{bf}} = c_0 - c_1\phi + c_2T - c_3\phi^2 - c_4\phi T + c_5\phi T^2 - c_6\phi^3 - c_7\phi^2 T + c_8\phi T^2 + c_9\phi T^3 + c_{10}\phi^4 + c_{11}\phi^3 T - c_{12}\phi^2 T^2 - c_{13}\phi T^3 \quad (4)$$

In the above equation, $(C_p)_{nf}$ represents the specific capacity of the nanofluid in kJ/kg K, $(C_p)_{bf}$ denotes the specific heat capacity of the base fluid in kJ/kg K, and C_0 to C_{13} represent the coefficients.

Table 2 lists the coefficients used in Eq. (4). Each coefficient (C_0 to C_{13}) has a corresponding value that is utilized in the equation.

Table 3 depicts the goodness of fit of Eq. (4). The goodness of fit is assessed through a sum of square errors of 0.0004077, an RMSE of 0.0028, and an R^2 value of 0.99884.

The fitting method yields residual errors ranging between 0.0004 and 0.0006, as depicted in Fig. 10.

Fig. 11 illustrates the error in estimating the SHC value for both the ANN and mathematical models. The error percentages for both methods are approximately ±0.45% and ±0.42%, which is in acceptable limit.

Fig. 12 depicts a comparison between the predicted and experimental SHC of the graphene/SAE10W oil NFs. According to the figures, both the ANN model and mathematical model predict SHC values that are consistent with experimental measurements.

Table 2 Coefficients of Eq. (4)

Coefficients	Value
C_0	1.5022
C_1	0.0273
C_2	0.0425
C_3	0.1110
C_4	0.0089
C_5	0.0054
C_6	0.0200
C_7	0.0056
C_8	0.0006
C_9	0.0001
C_{10}	0.0527
C_{11}	0.0042
C_{12}	0.0010
C_{13}	0.0008

Table 3 Goodness fit of Eq. (4)

SSE	R^2	RMSE
0.0004077	0.99884	0.0028

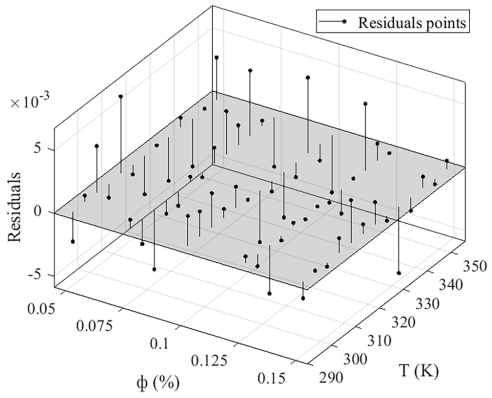

Fig. 10 Residuals plot for fitting

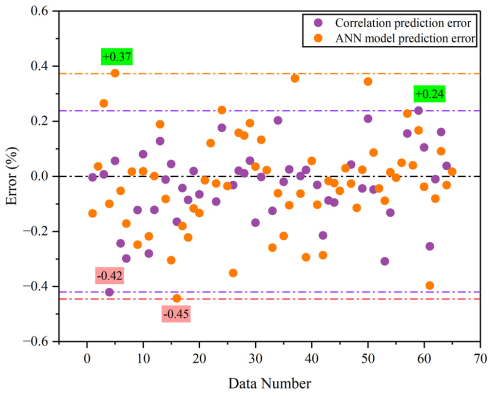

Fig. 11 Percentage of error in predicting SHC

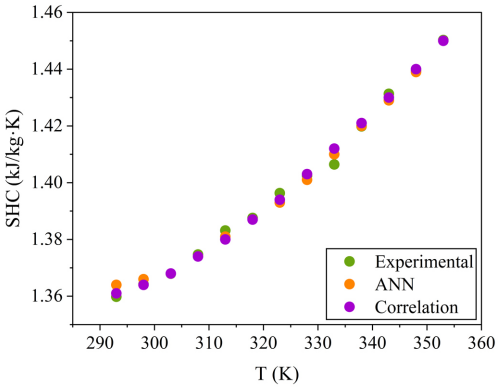

(e)

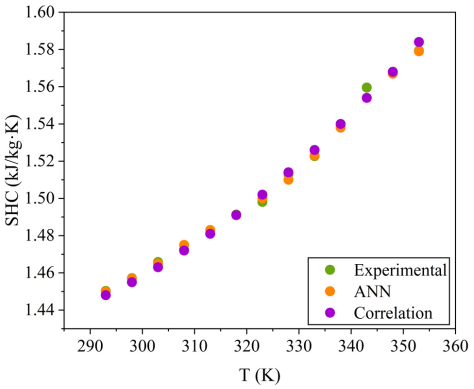

(c)

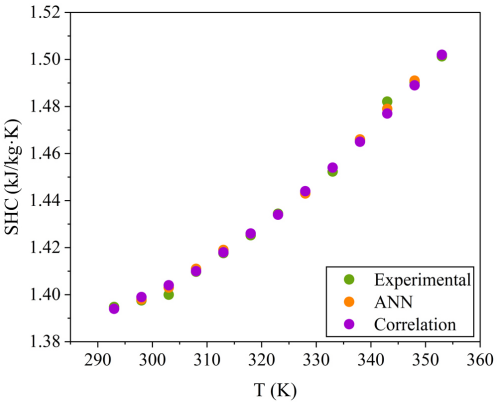

(d)

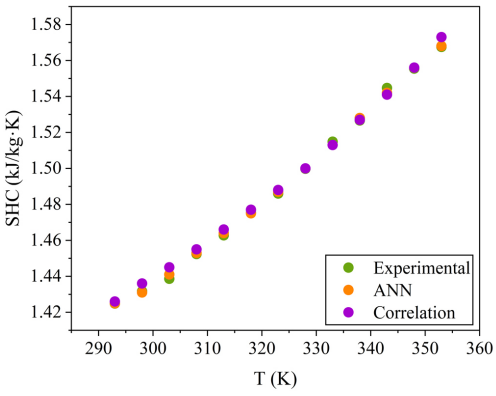

(b)

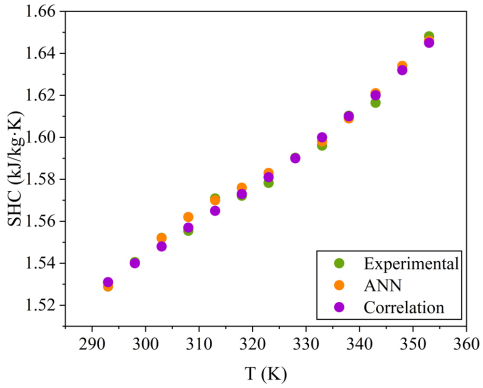

(a)

Fig. 12 Comparison of ANN and mathematical model outputs with experimental values a) Φ=0.050 v/v%, b) Φ=0.075 v/v%, c) Φ=0.100 v/v%, d) Φ=0.125 v/v%, e) Φ=0.150 v/v%

4 Conclusion

In this work, the specific heat capacity of graphene/SAE10W oil nanofluid was experimentally measured using a thermal constants analyzer. The experimental investigation was carried out based on volume concentrations of graphene nanoparticles in the SAE10W oil and fluid temperature between 293 K and 353 K. The experimental test results revealed the graphene/SAE10W oil nanofluids have a minimum reduction of SHC relative to the base fluid of 19% at 293 K with a graphene concentration of 0.050 v/v% and a maximum reduction of 40% at 353 K with a graphene concentration of 0.150 v/v%. Further, ANN and mathematical models were developed based on experimental data. The ANN model training results show a correlation coefficient and mean square error of 0.999 and 6.592×10^{-6}, respectively. The error percentages for both the ANN model and the mathematical model were ±0.45% and ±0.42%, respectively. The error rate for both techniques employed in the study of graphene/SAE10W oil nanofluids was less than ±0.45%. The results indicate these models predict the specific heat capacity of graphene/SAE10W oil nanofluids.

References

[1] Souza, R. R., Gonçalves, I. M., Rodrigues, R. O., Minas, G., Miranda, J. M., Moreira, A. L. N., Lima, R., Coutinho, G., Pereira, J. E., Moita, A. S. "Recent advances on the thermal properties and applications of nanofluids: From nanomedicine to renewable energies", Applied Thermal Engineering, 201, 117725, 2021. https://doi.org/10.1016/j.applthermaleng.2021.117725

[2] Said, Z., Sundar, L. S., Tiwari, A. K., Ali, H. M., Sheikholeslami, M., Bellos, E., Babar, H. "Recent advances on the fundamental physical phenomena behind stability, dynamic motion, thermophysical properties, heat transport, applications, and challenges of nanofluids", Physics Reports, 946, pp. 1–94, 2022. https://doi.org/10.1016/j.physrep.2021.07.002

[3] Younes, H., Mao, M., Murshed, S. M. S., Lou, D., Hong, H., Peterson, G. P. "Nanofluids: Key parameters to enhance thermal conductivity and its applications", Applied Thermal Engineering, 207, 2021, 118202, 2022. https://doi.org/10.1016/j.applthermaleng.2022.118202

[4] Nobrega, G., de Souza, R. R., Gonçalves, I. M., Moita, A. S., Ribeiro, J. E., Lima, R. A. "Recent developments on the thermal properties, stability and applications of nanofluids in machining, solar energy and biomedicine", Applied Sciences, 12(3), 2022. https://doi.org/10.3390/app12031115

[5] Kalsi, S., Kumar, S., Kumar, A., Alam, T., Dobrotă, D. "Thermophysical properties of nanofluids and their potential applications in heat transfer enhancement: A review", Arabian Journal Chemistry, 16(11), 2023. https://doi.org/10.1016/j.arabjc.2023.105272

[6] Srivastava, K., Sahoo, R. R. "Thermal, exergetic, and performance analysis of dissimilar-shaped nanoparticles hybrid nanofluid for flow across minichannel heat sink", Journal of Thermal Analysis and Calorimetry, 148(14), pp. 7501–7518, 2023. https://doi.org/10.1007/s10973-023-12191-4

[7] Alshuhail, L. A, Shaik, F., Sundar, L. S. "Thermal efficiency enhancement of mono and hybrid nanofluids in solar thermal applications – A review", Alexandria Engineering Journal, 68, pp. 365–404, 2023. https://doi.org/10.1016/j.aej.2023.01.043

[8] Maghrabie, H. M., Olabi, A. G., Sayed, E. T., Wilberforce, T., Elsaid, K., Doranehgard, M. H., Abdelkareem, M. A. "Microchannel heat sinks with nanofluids for cooling electronic components: Performance enhancement, challenges, and limitations", Thermal Science and Engineering Progress, 37, 101608, 2023. https://doi.org/10.1016/j.tsep.2022.101608

[9] Obalalu, A. M., Ahmad, H., Salawu, S. O., Olayemi, O. A., Odetunde, C. B., Ajala, A. O., Abdulraheem, A. "Improvement of mechanical energy using thermal efficiency of hybrid nanofluid on solar aircraft wings: an application of renewable, sustainable energy", Waves in Random and Complex Media, pp. 1–30, 2023. https://doi.org/10.1080/17455030.2023.2184642

[10] Patel, J., Soni, A., Barai, D. P., Bhanvase, B. A. "A minireview on nanofluids for automotive applications: Current status and future perspectives", Applied Thermal Engineering, 219, 119428, 2023. https://doi.org/10.1016/j.applthermaleng.2022.119428

[11] Ajeeb, W., Murshed, S. M. S. "Nanofluids in compact heat exchangers for thermal applications: A State-of-the-art review", Thermal Science and Engineering Progress, 30, 101276, 2022. https://doi.org/10.1016/j.tsep.2022.101276

[12] Li, J., Zhang, X., Xu, B., Yuan, M. "Nanofluid research and applications: A review", International Communications in Heat and Mass Transfer, 127, 105543, 2021. https://doi.org/10.1016/j.icheatmasstransfer.2021.105543

[13] Animasaun, I. L., Oke, A. S., Al-Mdallal, Q. M., Zidan, A. M. "Exploration of water conveying carbon nanotubes, graphene, and copper nanoparticles on impermeable stagnant and moveable walls experiencing variable temperature: thermal analysis", Journal of Thermal Analysis and Calorimetry, 148, pp. 4513–4522, 2023. https://doi.org/10.1007/s10973-023-11997-6

[14] Azharuddin, Saini, P. "Characterization, preparation and thermophysical properties investigations of aqueous $AgNO_3$–graphene hybrid nanofluids for heat transfer applications", International Journal of Thermophysics, 45, 2024. https://doi.org/10.1007/s10765-024-03377-5

[15] Rubaiee, S., Yahya, S. M., Fazal, M. A., Danish, M. "Characterization of Al_2O_3, TiO_2, hybrid Al_2O_3-TiO_2 and graphene oxide nanofluids and their performance evaluations in photovoltaic thermal system", Journal of Thermal Analysis and Calorimetry, 148, pp. 11467–11477, 2023. https://doi.org/10.1007/s10973-023-12492-8

[16] Adun, H., Wole-Osho, I., Okonkwo, E. C., Kavaz, D., Dagbasi, M. "A critical review of specific heat capacity of hybrid nanofluids for thermal energy applications", Journal of Molecular Liquids, 340, 116890, 2021. https://doi.org/10.1016/j.molliq.2021.116890

[17] Said, Z., Sharma, P., Elavarasan, R. M., Tiwari, A. K., Rathod, M. K. "Exploring the specific heat capacity of water-based hybrid nanofluids for solar energy applications: A comparative evaluation of modern ensemble machine learning techniques", Journal of Energy Storage, 54, 105230, 2022. https://doi.org/10.1016/j.est.2022.105230

[18] Gao, Y., Xi, Y., Yang, Z., Sasmito, A. P., Mujumdar, A. S., Wang, L. "Experimental investigation of specific heat of aqueous graphene oxide Al2O3 hybrid nanofluid", Thermal Science, 25(1), pp. 515–525, 2021. https://doi.org/10.2298/TSCI190404381G

[19] Zhang, Y. Xu, X. "Machine learning specific heat capacities of nanofluids containing CuO and Al2O3", AIChE Journal, 67(9), 2021. https://doi.org/10.1002/aic.17289

[20] Mukesh Kumar, P. C., Kavitha, R. "Regression analysis for thermal properties of Al_2O_3/H2O nanofluid using machine learning techniques", Heliyon, 6(6), e03966, 2020. https://doi.org/10.1016/j.heliyon.2020.e03966

[21] Kamsuwan, C., Wang, X., Piumsomboon, P., Pratumwal, Y., Otarawanna, S., Chalermsinsuwan, B. "Artificial neural network prediction models for nanofluid properties and their applications with heat exchanger design and rating simulation", International Journal of Thermal Sciences, 184, 107995, 2023. https://doi.org/10.1016/j.ijthermalsci.2022.107995

[22] Wang, X., Yan, X., Gao, N., Chen, G. "Prediction of thermal conductivity of various nanofluids with ethylene glycol using artificial neural network", Journal of Thermal Science, 29(6), pp. 1504–1512, 2020. https://doi.org/10.1007/s11630-019-1158-9

[23] Tian, S., Arshad, N. I., Toghraie, D., Eftekhari, S. A., Hekmatifar, M. "Using perceptron feed-forward artificial neural network (ANN) for predicting the thermal conductivity of graphene oxide-Al_2O_3/water-ethylene glycol hybrid nanofluid", Case Studies in Thermal Engineering 26, 101055, 2021. https://doi.org/10.1016/j.csite.2021.101055

[24] Sharma, P., Ramesh, K., Parameshwaran, R., Deshmukh, S. S. "Thermal conductivity prediction of titania-water nanofluid: A case study using different machine learning algorithms", Case Studies in Thermal Engineering 30, 101658, 2022. https://doi.org/10.1016/j.csite.2021.101658

[25] Ibrahim, M., Algehyne, E. A., Saeed, T., Berrouk, A. S., Chu, Y. M. "Study of capabilities of the ANN and RSM models to predict the thermal conductivity of nanofluids containing SiO_2 nanoparticles", Journal of Thermal Analysis and Calorimetry, 145, pp. 1993–2003, 2021. https://doi.org/10.1007/s10973-021-10674-w

[26] Alkanhal, T. A. "Comprehensive investigation of reduced graphene oxide (rGO) in the base fluid: thermal analysis and ANN modeling", Journal of Thermal Analysis and Calorimetry, 144, pp. 2605–2614, 2021. https://doi.org/10.1007/s10973-020-10433-3

[27] Olumegbon, I. A., Alade, I. O., Sahaluddin, M., Oyedeji, M. O., Sa'ad, A. U. "Modelling the viscosity of carbon-based nanomaterials dispersed in diesel oil: a machine learning approach", Journal of Thermal Analysis and Calorimetry, 145, pp. 1769–1777, 2021. https://doi.org/10.1007/s10973-020-10491-7

[28] Meijuan, C. "Application of ANN technique to predict the thermal conductivity of nanofluids: a review", Journal of Thermal Analysis and Calorimetry, 145, pp. 2021–2032, 2021. https://doi.org/10.1007/s10973-021-10775-6

[29] MATLAB "Neural Net Fitting, (R2023b)", Available at SRM Institute of Science and Technology, [computer program] Available at: https://matlab.mathworks.com/ [Accessed: 22 February 2024]

[30] Çolak, A. B., Yıldız, O., Bayrak, M., Tezekici, B. S. "Experimental study for predicting the specific heat of water based Cu-Al_2O_3 hybrid nanofluid using artificial neural network and proposing new correlation", International Journal of Energy Research, 44(9), pp. 7198–7215, 2020. https://doi.org/10.1002/er.5417

[31] Zhao, A. Z., Garay, J. E. "High temperature liquid thermal conductivity: A review of measurement techniques, theoretical understanding, and energy applications", Progress in Materials Science, 139, 101180, 2023. https://doi.org/10.1016/j.pmatsci.2023.101180

[32] Tiwari, A. K., Pandya, N. S., Shah, H., Said, Z. "Experimental comparison of specific heat capacity of three different metal oxides with MWCNT/ water-based hybrid nanofluids: proposing a new correlation", Applied Nanoscience, 13, pp. 189–199, 2023. https://doi.org/10.1007/s13204-020-01578-6

[33] Bakthavatchalam, B., Habib, K., Saidur, R., Saha, B. B., Irshad, K. "Comprehensive study on nanofluid and ionanofluid for heat transfer enhancement: A review on current and future perspective", Journal of Molecular Liquids, 305, 112787, 2020. https://doi.org/10.1016/j.molliq.2020.112787